Monodispersed Mesoporous Silica Nanoparticles with Very Large Pores for Enhanced Adsorption and Release of DNA

ARTICLE *in* THE JOURNAL OF PHYSICAL CHEMISTRY B · FEBRUARY 2009

Impact Factor: 3.3 · DOI: 10.1021/jp807956r · Source: PubMed

Monodispersed Mesoporous Silica Nanoparticles with Very Large Pores for Enhanced Adsorption and Release of DNA

Fei Gao,[†,‡] Pablo Botella,[*,†] Avelino Corma,[*,†] Jose Blesa,[§] and Lin Dong[‡]

Instituto de Tecnología Química, UPV-CSIC, Avenida Los Naranjos s/n, 46022 Valencia, Spain, Key Laboratory of Mesoscopic Chemistry of MOE, School of Chemistry and Chemical Engineering, Nanjing University, 210093 Nanjing, People's Republic of China, and Instituto de Biomedicina de Valencia, CSIC, Unitat de Genètica Molecular, c/Jaime Roig 11, 46010 Valencia, Spain

Received: September 8, 2008; Revised Manuscript Received: November 28, 2008

Silica nanoparticles with controlled diameter (∼70−300 nm) and with uniform pores of 20 nm are prepared by a low temperature (10 °C) synthetic method in the presence of a dual surfactant system. While a triblock copolymer (Pluronic F127) acts as supramolecular template and coassembles with hydrolyzed silica species to develop a partially ordered mesophase with face-centered cubic symmetry, a fluorocarbon surfactant with high surface activity (FC-4) surrounds the silica particles through $S^+X^-I^+$ interactions, thereby limiting their growth. The final textural properties of this material are achieved by means of a subsequent hydrothermal treatment to yield high pore volume mesoporous silica nanoparticles with the largest pore entrance size (17 nm) and cavity diameter (20 nm) reported up to now. After surface modification with aminopropyl groups, the nanoparticles are able to encapsulate inside the pores molecules of the firefly luciferase plasmid DNA (pGL3-Control, 5256 pb), leading to stable conjugates with up to 0.07 μg DNA m^{-2}, which is the highest content achieved with silica-based materials. Furthermore, plasmid DNA becomes protected from enzymatic degradation when conjugated with the mesostructured nanoparticles.

Introduction

Since the synthesis of mesoporous M41S materials,[1,2] advances in the synthesis of mesoporous silica materials with controlled particle size, morphology, and porosity have made silica matrices highly attractive for a wide variety of nanotechnological applications such as adsorption, catalysis, sensing, and separation.[3−10] Moreover, the possibility to tailor structural and textural parameters of the mesoporous wall, while introducing numerous possibilities for particle functionalization, have made these materials potential vehicles for delivery and controlled release of guest molecules, like drugs and biomolecules.[11−13] In this sense, Lin et al. have reported the use of MCM-41-type mesoporous silica nanoparticles (MSN) for drug and gene delivery, showing that such MSN can be readily internalized in vitro by animal and plant cells without any citotoxicity.[14−16] However, owing to structural restrictions of MCM-41-type MSN, the largest pore diameter is in the order of 6 nm,[17] which limits their application as a carrier for adsorption and release of large molecules (i.e., proteins and nucleic acids). The intracellular delivery of genetic material by nanoparticulated systems is today a technical challenge. To do this, it would be of great interest to develop a nanosized mesoporous structure with pores large enough to accommodate proteins and nucleic acids.

Recently, a new strategy for the synthesis at low temperature of mesoporous silica with very large pores has been studied by Zhao et al.[18−20] These authors described the synthesis of the FDU-12 material with a face-cubic centered (fcc) structure (space group *Fm*3*m*), and very large pore diameter (up to 27 nm) and unit cell (up to 44 nm) by using a block copolymer and a swelling agent (i.e., 1,3,5-trimethylbenzene, TMB) as templates. Because of the presence of inorganic salts in the synthesis gel, the interactions of the silicate species with nonionic block copolymers is enhanced, resulting in a highly ordered material. Nevertheless, for the purpose of encapsulating and delivering plasmids into cell, one should prepare materials not only with large pore volume, but these should be built into silica nanoparticles with a regular size distribution, preferably in the range 100−300 nm. In that sense, first Sánchez et al.[21] and later Ying et al.[22] have reported that fluorocarbon-based surfactants present high surface activity and their enrichment at the particle periphery can be used to control the growth of mesoporous particles. Finally, Landry et al.[12] have shown that mesoporous materials functionalized with aminopropyl groups present advanced adsorption properties for DNA immobilization, due to their large surface areas and internal pore volume and a narrow pore size distribution.

Here, we report on a novel type of silica-based nanostructured material obtained by a low temperature synthetic pathway using a double surfactant system; a triblock copolymer, which acts as supramolecular template and coassembles with hydrolyzed silica species, was combined with a fluorocarbon surfactant that surrounds the silica particles through $S^+X^-I^+$ interactions thereby limiting their growth. This method allows a straightforward and fast growth of mesoporous silica nanoparticles, ranging from ∼70−300 nm, with a partially ordered structure and very large pore entrances (up to 17 nm) and cavities sizes (up to 20 nm). Furthermore, functionalization of these large pore mesoporous silica nanoparticles with aminopropyl groups allows adsorbing and stabilizing plasmid DNA with superior efficiency than other silica-based materials reported up to now.

* To whom correspondence should be addressed. E-mail: (P.B.) pbotella@itq.upv.es; (A.C.) acorma@itq.upv.es. Fax: (+34) 96-387-7809. Tel: (+34) 96-387-7800.
† Instituto de Tecnología Química, UPV-CSIC.
‡ Nanjing University.
§ Instituto de Biomedicina de Valencia, CSIC.

10.1021/jp807956r CCC: $40.75
Published on Web 01/16/2009

Experimental Section

Preparation of Large Pore Mesoporous Silica Nanoparticles (NS). Mesoporous silica nanoparticles with large pores were synthesized by using a block copolymer (Pluronic F127, Aldrich) and a fluorocarbon surfactant (FC-4, Yick-Vik) as internal and external templates, respectively. In a typical synthesis, 0.25 g of F127 and 0.70 g of FC-4 were dissolved in 30 mL of HCl aqueous solution (0.02 M), followed by the introduction of 0.20 g of 1,3,5-trimethylbenzene (TMB) into the solution. The mixture was stirred for 2 h at 15 °C. Then, 1.50 g of tetraethylorthosilicate (TEOS) was added to the solution and stirred for 24 h at 5−15 °C. The molar ratio of the reactants TEOS/F127/TMB/FC-4/HCl/H_2O was 1:0.0028:0.24:0.12:0.08:232. The solution along with the precipitate was then introduced into an autoclave and hydrothermally treated at 100−150 °C for 24 h. The as-prepared product was filtered and washed first with water and subsequently with ethanol and dried in air. When needed, a second hydrothermal treatment was carried out. In that case, 0.50 g of as-prepared product was added to a solution of 30 mL of HCl 2 M in an autoclave, and the mixture was heated at 140 °C for 48 h.

Template removal was done by microwaves-assisted digestion.[23] The as-prepared sample (0.40 g) was introduced into a Teflon vessel with 6 mL of HNO_3 (15 M) and 4 mL of H_2O_2 (9 M), and the mixture was treated in a microwaves oven MARS-5 at 800 W, 2245 MHz, and 220 V. The maximum temperature (150 °C) was held for 2 min. The solid was recovered by filtration, washed with water and ethanol, and finally dried overnight at room temperature under vacuum.

Preparation of Surface-Methylated Large Pore Mesoporous Silica Nanoparticles (mNS). The surfactant-containing material (0.30 g) was vacuum dried at 100 °C. Then, 2.70 mL of anhydrous toluene and 0.12 mL of dimethyldimethoxysilane (DMDMS) were added, and the mixture was refluxed in nitrogen for 1 h. After cooling down to room temperature, 2.70 mL of anhydrous toluene and 0.12 mL of triethylamine were incorporated, and the mixture was refluxed in nitrogen for an additional 2 h. The resulting suspension was filtered, washed first with toluene and subsequently with methanol, and dried overnight at 100 °C. Then, the template was removed by the microwaves-assisted digestion method.

Preparation of Amine-Derivatized Large Pore Mesoporous Silica Nanoparticles (NSa, mNSa). The as-synthesized material (0.30 g) was vacuum dried at 100 °C. Then, 15 mL of anhydrous toluene and 0.68 mL of (3-aminopropy)trimethoxysilane APTMS were introduced, and the mixture was refluxed in nitrogen for 24 h. The resulting suspension was filtered, washed with toluene and methanol, and dried overnight at 100 °C. Amine-derivatized materials have also been obtained from a sample of commercial silica nanoparticles (SNPa, Aldrich) and a sample of mesoporous MCM-41-like silica nanoparticles prepared according to the literature (MSNa).[24]

Materials Characterization. Liquid nitrogen adsorption isotherms were measured in a Micromeritics ASAP 2010 Flowsorb apparatus. Surface area calculations were carried out using the BET method, whereas the pore size distribution was calculated according to the BJH algorithm.[25]

Nanoparticle size measurements were conducted using a Zetasizer Nano ZS (Malvern Instruments Ltd.). Briefly, dried materials were resuspended in absolute ethanol at a concentration of 5 μg ml^{-1}, and measurements were performed at 25 and 173° scattering angle. The mean hydrodynamic diameter was determined by cumulative analysis.

Samples for transmission electron microscopy (TEM) were ultrasonically dispersed in ethanol and transferred to carbon-coated copper grids. TEM micrographs were collected in a Philips CM-10 microscope operating at 100 kV. Scanning electron microscopy (SEM) micrographs were collected in a JEOL 6300 microscope operating at 20 kV.

^{29}Si NMR spectra were recorded at room temperature under magic angle spinning (MAS) with a Bruker AV400 spectrometer. The single pulse ^{29}Si spectra were acquired using pulses of 3.5 μs corresponding to a flip angle of $3\pi/4$ rad and a recycle delay of 240 s. Spectra were recorded with a 7 mm Bruker BL-7 probe and at sample spinning rate of 5 kHz. The ^{29}Si spectra were referenced to tetramethylsilane (TMS).

Finally, carbon analysis (FISONS, EA 1108 CHNS-O) allowed us to control the remaining surfactant after the samples were microwaves digested (<0.5%) and the concentration of aminopropyl groups in the functionalized samples.

Preparation of DNA Conjugates. The plasmid DNA used (pGL3-Control vector, 5256 bp; Promega, Madison, WI) contains the luciferase gene of *Photinus pyralis* controlled by the immediate early promoter of the SV40 and by the late SV40 enhancer. The plasmid was prepared from *Escherichia coli* DH5α by standard procedures[26] and isolated by using the PureYield™ Plasmid Midiprep (Promega) following the manufacturer's instructions. Ten milligrams of the dried material was dispersed in 1 mL aqueous solution of the pGL3-Control vector with concentration ranging from 10 to 100 μg ml^{-1}. Details on the standard techniques followed for the amplification and purification of the plasmid can be found elsewhere.[14] The mixture was shaken at 1400 rpm and 25 °C for 24 h. Then, the sample was centrifuged at 12 000 rpm (27 610 g) for 10 min in order to ensure that all nanoparticles were removed from the solution. Supernatant was removed, and the sample was washed with 1 mL of sterile milli-Q water. Plasmid DNA (pDNA) content in the aqueous solutions was analyzed spectrophotometrically at 260 nm using a Nanodrop ND1000 spectrophotometer. The amount of plasmid adsorbed on materials was calculated by subtracting the pDNA content in the supernatants from the initial concentration. Triplicate samples were run for every experiment.

Stability Studies of pDNA-NS Conjugates. The complexation between pGL3-Control and NS materials were studied by agarose gel electrophoresis.[27−29] The as-prepared pDNA-NS conjugate was resuspended in sterile water at a pGL3-Control concentration of 0.2 μg/μL. Aliquots of 5 μL of this complex (containing 1 μg of pGL3-Control) were used for determining the electrophoretic shifts. When needed, the aliquot of pDNA-NS (5 μL) was digested with endonucleases *Bgl*II (1 U) and *Sal*I (1 U) at 37 °C overnight. Also when needed, pGL3-Control was extracted from the aliquot of pDNA-NS (5 μL) by vigorous agitation in NaCl 2 M aqueous solution at 50 °C for 30 min. This procedure was repeated three times and the supernatants from each sample were centrifuged at 14 000 rpm (37 580 g) and 4 °C for 15 min. The pDNA was ethanolic precipitated and resuspended in Tris-EDTA buffer. All the solutions were run on 0.8% agarose at 100 V for 2 h, subsequently stained with ethidium bromide, and documented by using a UV Bioimaging System (Isogen).

Results and Discussion

Large Pore Mesoporous Silica Nanoparticles. The synthesis of mesoporous materials at low temperature, by using mixed micelles of a block copolymer (F127) and a swelling agent (TMB) as structure directing agent, was formerly studied by

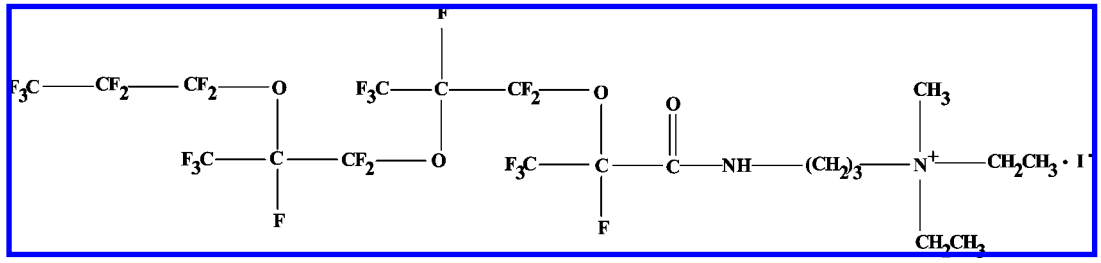

Figure 1. Structure of FC-4 surfactant.

TABLE 1: Textural Properties of NS Samples Prepared at Different Temperature[a]

sample	T_S[b] (°C)	T_{HT}[c] (°C)	T_{HT2}[d] (°C)	S_{BET} ($m^2\ g^{-1}$)	Vp ($cm^3\ g^{-1}$)	cavity size[e] (nm)	entrance size[f] (nm)
NS-1	15	135		561	0.87	12.2	5.3
NS-2	10	135		514	0.87	17.6	5.3
NS-3	5	135		447	0.73	17.4	6.3
NS-4	10	100		716	0.79	17.2	3.7
NS-5	10	150		403	0.80	17.5	7.1
NS-6	10	150	140	201	0.60	20.5	17.3

[a] Gel molar composition: 1 TEOS/0.0028 F127/0.24 TMB/0.12 FC-4/0.08 HCl/232 H_2O. [b] Synthesis temperature. [c] Temperature of the first hydrothermal treatment. [d] Temperature of the second hydrothermal treatment. [e] Calculated from the adsorption curve of the N_2 sorption isotherm, based on the BJH method.[25] [f] Calculated from the desorption curve of the N_2 sorption isotherm, based on the BJH method.[25]

Zhao et al.[18] Nevertheless, with the objective to generate materials for biological applications it is strongly required to go through a nanoparticulated system.[30] To achieve this and taking into account the potential of fluorocarbon surfactants for the control of particle size,[21,22] we have incorporated the surfactant FC-4 to the initial gel (Figure 1). Then, by working at 15 °C the NS-1 material was obtained, which was subjected to a further hydrothermal treatment at 135 °C (Table 1). The removal of the template was done by microwaves-assisted digestion. This method avoids the significant shrinkage related to surfactant thermal decomposition.[31,32] The TEM and SEM images given in Figure 2 show acceptably uniform, highly monodispersed spheroids with large pores. Particle size distribution ranges ~70−300 nm with a mean size of 150 ± 50 nm (Figure 3). This nanosized system does not present the excellent fcc mesostructure of the bulk FDU-12 material,[18−20] but due to the small particle size, large pore diameter, and spherical morphology, the pore ordering in a long-range is restricted and the cubic periodicity becomes distorted. In fact, it was not possible to obtain a clear electron diffraction spot of this material, as the number of unit cells in a single particle is very low. This is not surprising since such structural limitations have also been described for other submicronic spherical mesoporous materials.[33−36] Nevertheless, the system presented here differs from mesocellular foams with large pores,[22,37−39] because the nanoparticles retain some domains of the fcc symmetry (Figure 1a, inset).

The nitrogen sorption isotherm of NS-1 displays a type IV adsorption isotherm of mesoporous materials with a type H2 hysteresis loop (Figure 4a), corresponding to a cagelike pore structure connected by windows with smaller size.[18−20,40] BET surface and total pore volume are, 561 $m^2\ g^{-1}$ and 0.87 $cm^3\ g^{-1}$, respectively. We have also calculated the diameter of the cavity and the entrance size, respectively, from the adsorption and desorption curves of the isotherm, according to the BJH method. The diameter of the internal cavities is within a narrow distribution with a mean diameter of 12.2 nm (Figure 4b), suggesting a uniform mesopore size. However, the size of the external windows is more heterogeneous with a dual distribution centered at 5.3 and 3.6 nm (Figure 3c). Besides this, NS-1 material shows some interparticle (textural) porosity, as evidenced by the adsorption step at high relative pressures ($p/p_0 > 0.9$).

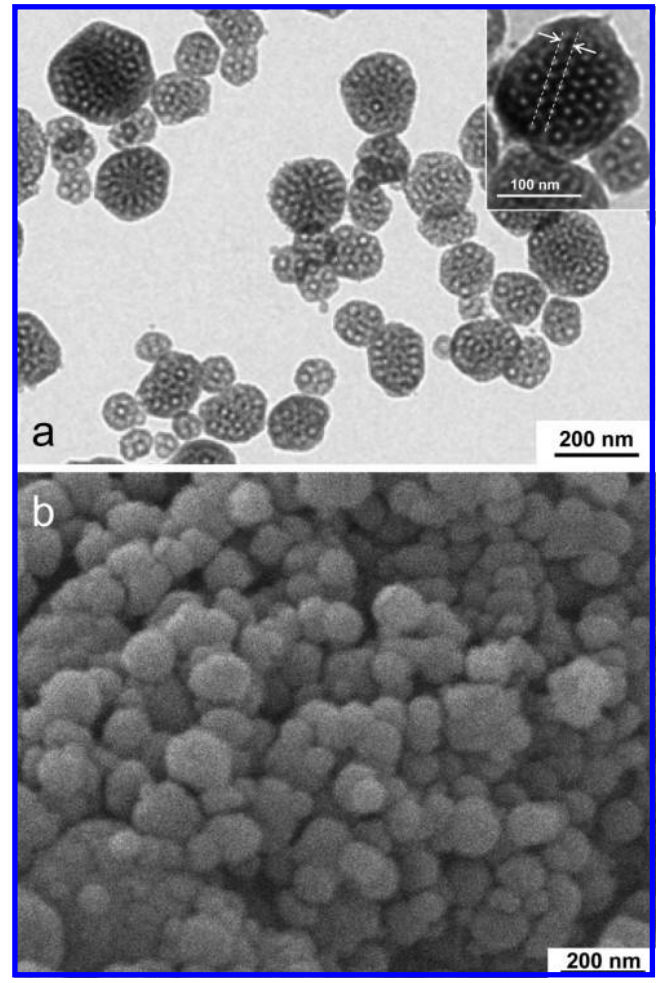

Figure 2. (a) TEM image of large pore mesoporous silica nanoparticles synthesized at 15 °C with a hydrothermal treatment at 135 °C (NS-1); the inset shows the view from [110] direction and local arrangement. (b) SEM image of this sample.

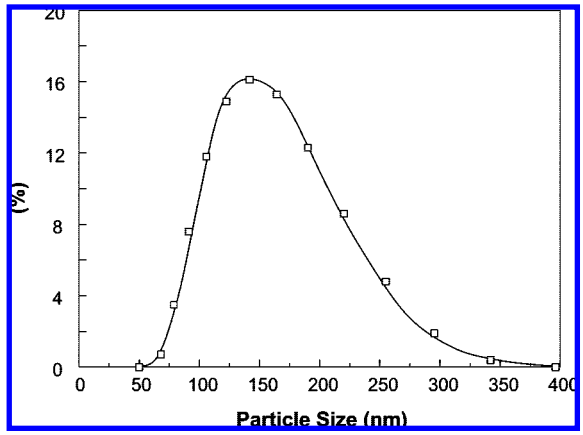

Figure 3. Nanoparticle size distribution of NS-1 synthesized at 15 °C with a hydrothermal treatment at 135 °C; the mean hydrodynamic diameter is about 150 ± 50 nm.

At this point, the material produced was not adequate for our purpose since the diameter of the pore entrance and cavities was still too small. Then, the synthesis conditions were further explored. More specifically, when the synthesis temperature was decreased to 10 and 5 °C, samples NS-2 and NS-3 were obtained and the resultant N_2 adsorption isotherms were still of the type IV with a type H2 hysteresis loop (Figure 5a), indicating cagelike mesopores similar to those obtained at 15 °C. High BET surface area and pore volume are also present in these materials. However, the p/p_0 at the point of capillary condensation increases from 0.87 for NS-1 to 0.9 for NS-2 and NS-3, corresponding to an expansion of the cavity size up to 17.4 nm (Table 1). This is due to the favored swelling of TMB molecules within the F127 micelles at a relatively lower temperature.[18] At the same time, TEM images of the NS-3 material show the presence of some small amorphous silica spheres growing among the large pore mesostructured nanoparticles (Figure 5b). Here, it must be taken into account that when the synthesis temperature is lower than the critical micelle temperature (CMT), no interaction takes place between block copolymers and silicate species and thus, no mesoporous structure is formed.[41,42] In our case, it was possible to obtain a partially ordered mesoporous material even at a temperature as low as 5 °C, although at this temperature we are probably very close to the collapse of the mesostructure.

Nevertheless, this was a step forward for our objective, since for transportation and diffusion of large molecules (i.e., proteins and nucleic acids) in mesoporous materials, a wide pore entrance will favor the process. Thus, we have further modified the hydrothermal treatment temperature for synthesizing a material with still larger pore entrance. It has been shown that temperature in nonionic triblock copolymer templated systems allows the control of the pore diameter expansion without significant influence on the wall thickness.[37−39,43] Then, we have hydrothermally post-treated the material synthesized at temperatures in the range 100−150 °C. Samples obtained after hydrothermal treatment at 100 and 150 °C (NS-4 and NS-5, respectively) show the same type of N_2 sorption isotherm than NS-2 material (Figure 6) but with smaller hysteresis loops, as a consequence of the enlargement of the pore entrance up to 7.1 nm (Figure 6c). Conversely, the cavity size does not show any significant change when increasing the temperature of the hydrothermal treatment (Figure 6b). A further expansion of pore entrance was achieved by a second hydrothermal treatment at 140 °C. At this point, the as-prepared material at 150 °C was introduced again into an autoclave and hydrothermally treated at 140 °C for 48 h. The obtained sample (NS-6) shows a different pattern of N_2 sorption isotherm with a H1 type hysteresis loop, corresponding to an increase of the entrance size up to 17.3 nm (Figure 6c, Table 1). Moreover, the cavity size shows also a small expansion (about 17%) from sample NS-5 (17.5 nm) to NS-6 (20.5 nm). A consequence of the increase in pore entrance and cavity sizes is that the BET surface area decreases from 716 (NS-4) to 201 $m^2\ g^{-1}$ (NS-6) (Table 1).

From TEM images of sample NS-6, a pore diameter of ∼20 nm can be estimated in accordance with the N_2 sorption measurements (Figure 7). To our knowledge, this is the largest pore size reported in a nanosized mesoporous material. Indeed, Ying et al. have described the synthesis of a nanoparticulated mesocellular foam with average pore size of 19.5 nm.[22] Such value, provided from the adsorption curves of the N_2 isotherm, corresponds to the internal cavities developed within the nanoparticles. Although no data is given for the pore entrance size of this material, it presents a large hysteresis loop, which indicates a strong reduction of pore diameter at the entrances of those cavities. It is also noteworthy that in our case the fcc symmetry is still present even in the smallest nanoparticles (∼100 nm) with pores of 20 nm, thus showing the high stability of this material (Figure 6, inset). Different authors have shown that when pore size and cell parameter are greatly enlarged the mesostructured system turns into a disordered mesocellular foam material.[22,37−39] Conversely, Zhao et al.[18−20,40] have introduced inorganic salts during the synthesis gel to enhance the interaction of silicate species with nonionic block copolymers, resulting in a highly ordered large pore FDU-12 material. In our case, inorganic salts were not required to form a defined mesophase in the nanoparticles, since the weakly acidic synthesis conditions promote a slow hydrolysis of silica precursors that allows the coassembling of the surfactant molecules and organic additives,[19] while the fluorocarbon surfactant can also stabilize this system.

Advanced Adsorption of DNA on NS Materials. Silica-based nanosized materials with cationic groups have been so far reported to electrostatically bind DNA molecules and to undergo gene delivery successfully.[27,28,44−47] However, the uptake of DNA is limited by a relatively low external surface area. In this sense, mesoporous materials show outstanding textural properties that can improve the performance in DNA immobilization.[48] Landry et al.[12] have pointed out the advantage of widening the size of the pore entrances of functionalized mesoporous materials as a route to enhance the performance of the adsorption process. Therefore, we have prepared and characterized an aminopropyl-derivatized NS-5 material (sample NS-5a).

The nitrogen sorption isotherm and the corresponding textural properties of NS-5a are shown in Table 2 and Figure 8. The amine-derivatized material retains the type IV adsorption isotherm of the original mesoporous materials with a type H2 hysteresis loop, but a significant reduction of surface area and total pore volume takes place, together with a slight reduction of the diameter of the cavity and pore entrance, due to the presence of the attached functional groups. ^{29}Si-MAS NMR spectrum confirmed the modification of the silica surface with the silane linker (figure not shown). Besides the typical resonances at −92.1, −102.2, and −111.5 ppm, which are assigned to Q_2 ($[Si(OSi)_2(OH)_2]$), Q_3 ($[Si(OSi)_3(OH)]$), and Q_4 ($[Si(OSi)_4]$) species, respectively,[49,50] T_2 ($[Si(OSi)_2(OH)(R)]$) and T_3 ($[Si(OSi)_3(R)]$) signals with shifts of −59.8 and −68.3 ppm, are clearly seen, indicating that the organic linker was successfully attached to the parent material. Moreover, according to carbon analysis, NS-5a presents 1.7 mmol linker g^{-1} (Table 2).

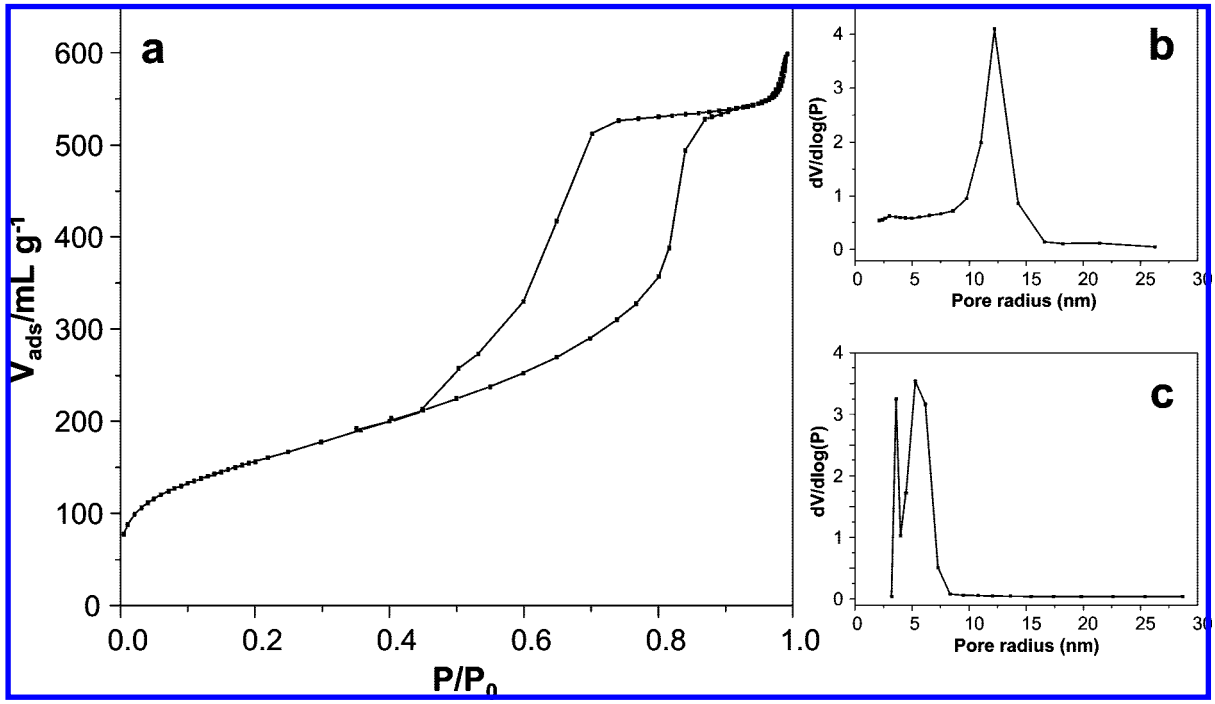

Figure 4. Nitrogen sorption isotherms (a), cavity sizes distribution (b), and pore entrance sizes distribution (c) of NS-1 sample synthesized at 15 °C with a hydrothermal treatment at 135 °C.

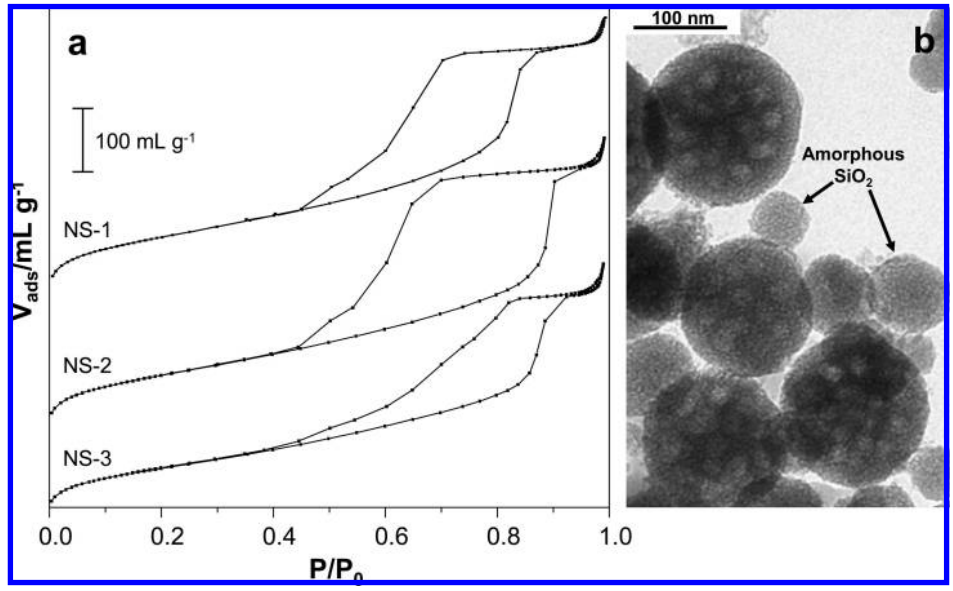

Figure 5. (a) Nitrogen sorption isotherms of samples synthesized at 15 °C (NS-1), 10 °C (NS-2), or 5 °C (NS-3) with a hydrothermal treatment at 135 °C. (b) TEM image of NS-3 sample showing some amorphous silica nanoparticles.

When contacting the NS-5a material with an aqueous solutions of pDNA with concentrations ranging from 10 to 100 μg ml^{-1} at 25 °C, the amount of adsorbed nucleic acid into the pores increases when increasing the pDNA concentration (Figure 9), with a maximum loading of 5.1 μg pDNA mg^{-1}. No pDNA adsorption occurred in the corresponding nonfunctionalized material.

The effectiveness of NS-5a for enhanced pDNA adsorption has been compared with the following aminopropyl-silica-based nanosized materials: (i) commercial silica nanoparticles (SNPa, average particle diameter = 10 nm), and (ii) mesoporous silica nanoparticles (MSNa, average particle diameter = 100 nm). The chemical and textural properties of these samples are presented in Table 2. SNPa and MSNa samples were contacted in a 100 μg ml^{-1} aqueous solution of pDNA at 25 °C, retaining, respectively, 2.8 and 4.3 μg pDNA mg^{-1}. It is noteworthy that NS-5a is able to incorporate more pDNA molecules than any other silica-based material even with a lower level of functionalization. However, after normalization to the surface area of each sample, NS-5a has the highest extent of modification (7.8 μmol linker m^{-2}). It must be taken into account that the estimated molecular diameter for the adsorbed pGL3-Control plasmid is about 550 nm in an extended conformation, which is strongly reduced when the plasmid takes a supercoiled configuration.[51,52] However, even in this last case, the size of the plasmid can be too large to accommodate on the surface of very small SNP or within the medium-pore channels of standard MCM-41-like materials, thus, presenting serious restrictions to diffuse inside the pores, and piling on the external surface.[12] In contrast, NS-5a, with enlarged pore entrance and cavity sizes,

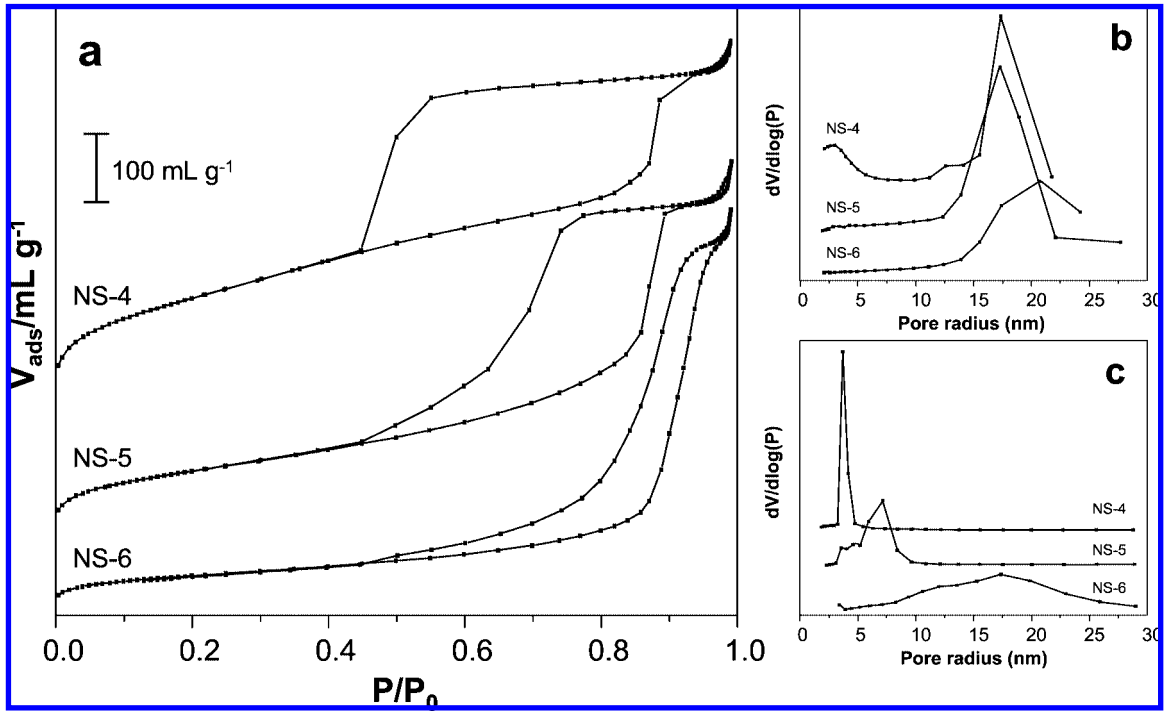

Figure 6. Nitrogen sorption isotherms of samples synthesized at 10 °C with a hydrothermal treatment at 100 °C (NS-4), 150 °C (NS-5) or a double hydrothermal treatment (150 and 140 °C) (NS-6). (b) cavity sizes distribution of the same samples; (c) pore entrance sizes distribution of the same samples.

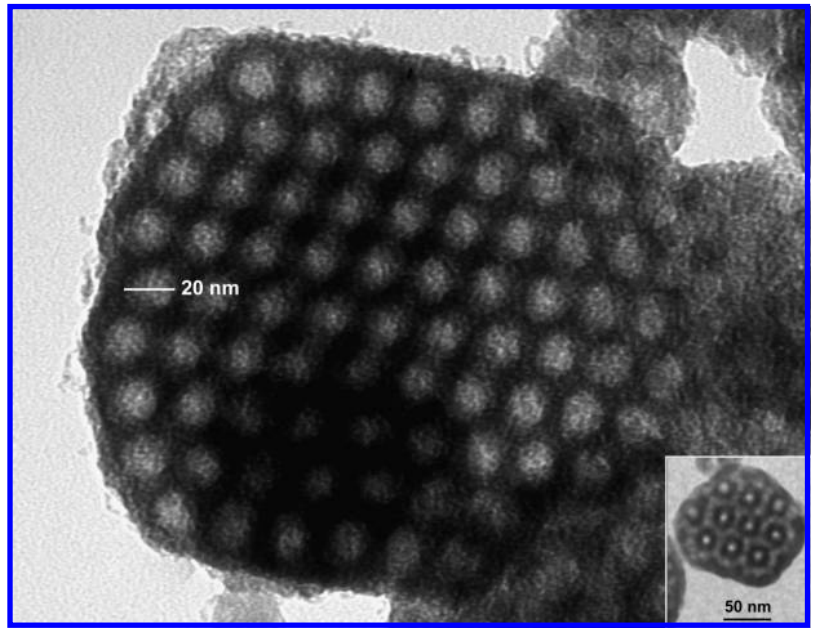

Figure 7. (a) Detail of very large pores in NS-6 synthesized at 10 °C with a double hydrothermal treatment (150 and 140 °C); the inset shows the local arrangement of fcc symmetry in a small particle.

is able to incorporate the plasmid molecules within the mesoporous structure. This has been further confirmed by removing the functional groups on the external surface of the NS-5a nanoparticles. For this purpose, a severe methylation treatment was performed on the as-synthesized, surfactant-containing, NS-5 material, thus blocking most of external silanol groups (sample mNS-5). The extension of methylation can be appreciated in the solid-state ^{29}Si MAS NMR of the modified sample (Figure 10), which shows only the D_2 ($[Si(OSi)_2(CH_3)_2]$) resonance at −16.2 ppm, corresponding to the successful attachment of the organic linker to the parent material. After template removal in mNS-5 sample, the internal silanols were functionalized with aminopropyl groups (sample mNS-5a). As expected, a lower quantity of the linker was grafted on the material with methylated surface (1.5 mmol linker g^{-1}). However, this sample is still able to adsorb a high amount of pDNA (3.9 μg mg^{-1}), thus showing that most of the adsorption occurs inside the mesopores of the nanoparticles. Conversely, methylated derivatives of SNP and MSN materials incorporated negligible quantities of pDNA.

According to this, by enlarging the cavity size and specially the pore entrance diameter of NS materials, one should expect even better results for the adsorption step. Indeed, several authors have reported on the benefit of widening the pore size

TABLE 2: Chemical and Textural Properties of Aminopropyl-Modified SNP, MSN, and NS Samples

sample	S_{BET} (m^2 g^{-1})	Vp (cm^3 g^{-1})	cavity size[a] (nm)	entrance size[b] (nm)	Si-R-NH_2[c] (mmol g^{-1})	pGL3 adsorption[d] (μg g^{-1})
SNPa[e]	52				3.0	2.8 ± 0.2
MSNa[f]	871	0.56	3.5		2.2	4.3 ± 0.1
NS-5a	212	0.51	15.5	5.7	1.7	5.1 ± 0.2
mNS-5a	252	0.50	15.5	4.2	1.5	3.9 ± 0.3
NS-6a	135	0.46	20.3	17.2	1.3	9.7 ± 0.2

[a] Calculated from the adsorption curve of the N_2 sorption isotherm, based on the BJH method.[25] [b] Calculated from the desorption curve of the N_2 sorption isotherm, based on the BJH method.[25] [c] Calculated from carbon analysis. [d] pGL3-control adsorption from 1 mL of a 100 μg ml^{-1} aqueous solution on 10 mg of material at 25 °C. Triplicate samples were run for every experiment (mean ± standard deviation). [e] Parent SNP: $S_{BET} = 578$ m^2 g^{-1}. [f] Parent MSN: $S_{BET} = 1048$ m^2 g^{-1}; Vp = 0.63 cm^3 g^{-1}; pore diameter = 3.8 nm.

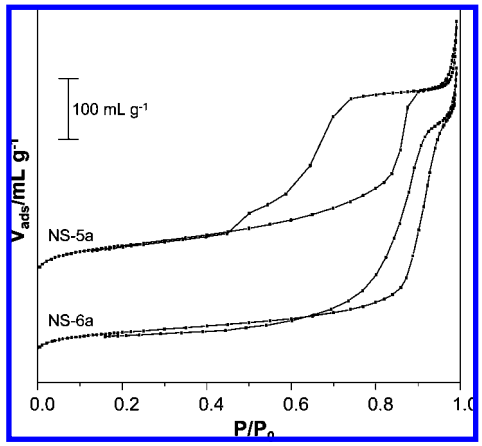

Figure 8. Nitrogen sorption isotherms of aminopropyl-modified samples synthesized at 10 °C with a hydrothermal treatment at 150 °C (NS-5a) or a double hydrothermal treatment (150 and 140 °C) (NS-6a).

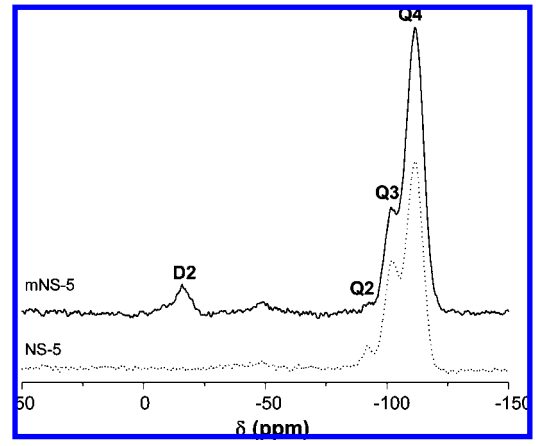

Figure 10. ^{29}Si-MAS NMR spectra of NS-5 synthesized at 10 °C with a hydrothermal treatment at 150 °C and mNS-5 synthesized at 10 °C with a hydrothermal treatment at 150 °C and further methylation of surface.

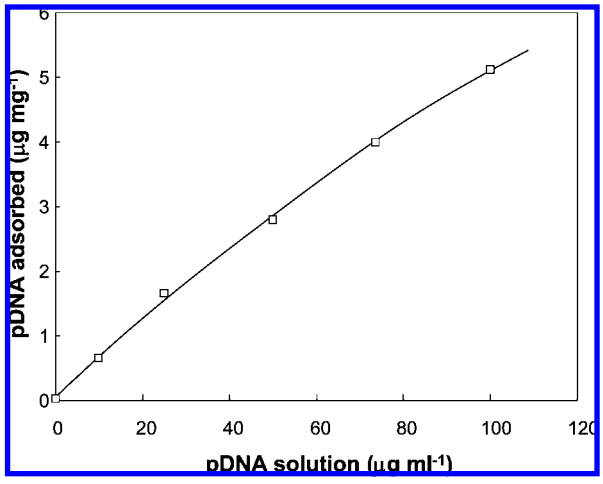

Figure 9. pGL3-Control adsorption isotherm (25 °C) of aminopropyl-modified sample synthesized at 10 °C and with a hydrothermal treatment at 150 °C (NS-5a).

of mesoporous materials for bioimmobilization proccesses,[12,17,40,53−56] For this reason, an aminopropyl-derivatized NS-6 material has been prepared and characterized (sample NS-6a) and its chemical and textural properties are presented in Table 2 and Figure 8. It can be seen there that the postsynthesis modification of the silica with the aminopropyl linker has negligible effects on the effective pore diameter and pore volume of the material. When contacting with a 100 μg ml^{-1} aqueous solution of pDNA with this sample at 25 °C, a maximum loading of 9.7 μg mg^{-1} (97% of starting pDNA) was achieved. This material is able to adsorb more DNA per unit surface area than any other reported up to now (0.07 μg m^{-2}).[12] Furthermore, due to the large pore entrance and cavity sizes of NS-6a, intermolecular interactions among pDNA molecules are expected to be minimized, and then no diffusion limitations in and to outside the mesoporous structure can be expected. This has been confirmed by contacting the pDNA-containing sample in a 2 M NaCl aqueous solution at 50 °C for 30 min, as more than 95% of adsorbed pDNA was released from the nanoparticles. Nevertheless, we are aware that the small particle size of this material can also play an important role in the diffusion of DNA molecules. As shown by Zhao et al.,[57] mesoporous silicas with smaller particles posess more entrances for diffusion of bulky molecules than conventional materials with large particle size. This avoids molecular diffusion blocking due to localized multilayer adsorption and favors the fast desorption of DNA molecules.

To study the stability of the pGL3-NS-6a conjugate at physiological conditions, agarose gel electrophoresis was run for 2 h at 100 V in a 0.8% gel stained with ethidium bromide. Figure 11 shows the electrophoretic shifts for pGL3-Control in the absence and in the presence of NS-6a. The results demonstrate the stability of the conjugates pDNA-NS, as illustrated by the retention of pGL3-Control around the sample well (lane 4). However, pGL3-Control can be released from its complex with NS-6a by vigorous agitation in 2 M NaCl (aq), thus showing no change in the electrophoretic pattern relative to the free plasmid (lanes 2 and 6). To assess stability against enzymatic digestion, the uncomplexed plasmid and the conjugate pGL3-NS6a were incubated with *Bgl*II and *Sal*I endonucleases, followed by deactivation of the enzymes at 70 °C. These enzymes cut the plasmid (5256 bp) at positions 36 and 2448, respectively, producing two fragments of 2413 bp and 2843 bp. Alternatively, after enzymatic digestion pGL3-Control can be extracted from its conjugate with NS-6a with a 2 M NaCl (aq).

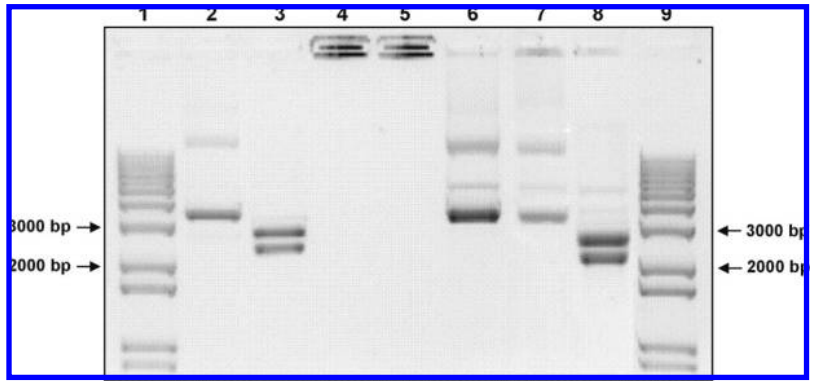

Figure 11. Agarose gel electrophoresis showing protection of pDNA from endonucleases when is complexed with NS samples. Lanes 1 and 9, DNA marker (1 kb Plus; Invitrogen); lane 2, undigested free pDNA (pGL3-Control); lane 3, free pGL3-Control after digestion with *Bgl*II and *Sal*I; lane 4, pGL3-NS6a conjugate; lane 5, the pGL3-NS6a conjugate digested with *Bgl*II and *Sal*I; lane 6, the pGL3-Control extracted from pGL3-NS6a conjugate with 2 M NaCl; lane 7, the pGL3-Control extracted from pGL3-NS6a conjugate with 2 M NaCl after digestion with *Bgl*II and *Sal*I; lane 8, the pGL3-Control extracted from pGL3-NS6a conjugate with 2 M NaCl and subsequently digested with *Bgl*II and *Sal*I.

Free pDNA was digested and cleaved by both enzymes (lane 3), while the complex pGL3-NS6a was not affected under the same conditions and the electrophoretic shift of the released pDNA was the same that the free plasmid (lanes 5 and 7), suggesting that the system pGL3-NS6a is able to protect DNA from enzymatic cleavage. This protection against enzymatic digestion can be due to a hindered access of the enzymes to the pDNA immobilized in the mesoporous structure, no matter if it is located on the external surface or at the inner cavities,[45] but also to a conformational change in pDNA that makes it impossible or at least quiet slow the cleavage.[28] Such protection is not further effective if the pDNA is released from the conjugate pGL3-NS6a before incubation with the endonucleases (lane 8).

Conclusions

The synthesis of mesoporous silica nanoparticles (∼70−300 nm) with very large regular pores has been achieved by controlling the following parameters: (i) synthesis temperature (10 °C), which allows the building of high diameter internal cavities; (ii) high temperature of the subsequent hydrothermal treatment (150 °C), which allows the development of wide opened windows on the external surface of the mesostructure that communicate with the internal cavities; and (iii) a dual surfactant system: a nonionic block copolymer (F127) to build the mesophase and a fluorocarbon surfactant with high surface activity (FC-4) to control the crystallite growth, leading to nanoparticles. By optimizing the above synthesis parameters, it was possible to synthesize mesoporous silica nanoparticles with partially ordered fcc symmetry, high pore volume, and very large pore entrance size (up to 17 nm) and cavity diameter (up to 20 nm). After surface modification with aminopropyl groups, very high adsorption of pDNA molecules inside the mesophase can take place. The stability of pDNA-NS conjugates offers protection for enzymatic degradation. Currently, studies on specific cellular targeting and pDNA uptake are in process.

Acknowledgment. The authors thank CICYT (MAT2006-14274-C02-01) and Generalitat Valenciana (GV05/173) for financial support and the Electronic Microscopy Service of UPV for technical support. F.G. also thanks the Chinese Scholarship Council (CSC) for a predoctoral fellowship (State-Sponsored Graduate Scholarship Program for Building High-Level Universities).

References and Notes

(1) Beck, J. S.; Vartuli, J. C.; Roth, W. J.; Leonowicz, M. E.; Kresge, C. T.; Schmitt, K. D.; Chu, C. T. W.; Olson, D. H.; Sheppard, E. W.; McCullen, S. B.; Higgins, J. B.; Schlenker, A. *J. Am. Chem. Soc.* **1992**, *114*, 10834.

(2) Kresge, C. T.; Leonowicz, M. E.; Roth, W. J.; Vartuli, J. C.; Beck, J. S. *Nature* **1992**, *359*, 710.

(3) Huh, S.; Wiench, J. W.; Yoo, J.-C.; Pruski, M.; Lin, V. S. Y. *Chem. Mater.* **2003**, *15*, 4247.

(4) Trewyn, B. G.; Whitman, C. M.; Lin, V. S. Y. *Nano Lett.* **2004**, *4*, 2139.

(5) Suzuki, K.; Ikari, K.; Imai, H. *J. Am. Chem. Soc.* **2004**, *126*, 462.

(6) Ying, J. Y. *Chem. Eng. Sci.* **2006**, *61*, 1540.

(7) Ying, J. Y.; Mehnert, C. P.; Wong, M. S. *Angew. Chem., Int. Ed.* **1999**, *38*, 56.

(8) Corma, A. *Chem. Rev.* **1997**, *97*, 2373.

(9) Corma, A.; Jordá, J. L.; Navarro, M. T.; Rey, F. *Chem. Commun.* **1998**, 1899.

(10) Corma, A.; Díaz-Cabañas, M. J.; Moliner, M.; Rodríguez, G. *Chem. Commun.* **2006**, 3317.

(11) Vallet-Regí, M.; Balas, F.; Arcos, D. *Angew. Chem., Int. Ed* **2007**, *46*, 7548.

(12) Landry, C. C.; Solberg, S. M. *J. Phys. Chem. B* **2006**, *110*, 15261.

(13) Corma, A.; Moliner, M.; Díaz-Cabañas, M. J.; Serna, P.; Femenia, B.; Primo, J.; García, H. *New. J. Chem.* **2008**, *32*, 1338.

(14) Slowing, I. I.; Vivero-Escoto, J. L.; Wu, C.-W.; Lin, V.S.-Y. *Adv. Drug Delivery Rev.* **2008**, *60*, 1278.

(15) Slowing, I. I.; Trewyn, B. G.; Giri, S.; Lin, V. S.-Y. *Chem. Commun.* **2007**, 3236.

(16) Slowing, I. I.; Trewyn, B. G.; Giri, S.; Lin, V. S.-Y. *Adv. Funct. Mater.* **2007**, *17*, 1225.

(17) Slowing, I. I.; Trewyn, B. G.; Lin, V. S.-Y. *J. Am. Chem. Soc.* **2007**, *129*, 8845.

(18) Fan, J.; Yu, C.; Lei, J.; Zhang, Q.; Li, T.; Tu, B.; Zhou, W.; Zhao, D. *J. Am. Chem. Soc.* **2005**, *127*, 10794.

(19) Zhou, X.; Qiao, S.; Hao, N.; Wang, X.; Yu, C.; Wang, L.; Zhao, D.; Lu, G. Q. *Chem. Mater.* **2007**, *19*, 1870.

(20) Yu, T.; Zhang, H.; Yan, X.; Chen, Z.; Zou, X.; Oleynikov, P.; Zhan, D. *J. Phys. Chem. B* **2006**, *110*, 21467.

(21) Areva, S.; Boissière, C.; Grosso, D.; Asakawa, T.; Sanchez, C.; Lindén, M. *Chem. Commun.* **2004**, 1630.

(22) Han, Y.; Ying, J. Y. *Angew. Chem., Int. Ed.* **2005**, *44*, 288.

(23) Tian, B.; Liu, X.; Yu, C.; Gao, F.; Luo, Q.; Xie, S.; Tu, B.; Zhao, D. *Chem. Commun.* **2002**, 1186.

(24) Cai, Q.; Luo, Z.-S.; Pang, W.-Q.; Fan, Y-W.; Chen, X.-H.; Cui, F.-Z. *Chem. Mater.* **2001**, *13*, 258.

(25) Barrett, E. P.; Joyner, L. S.; Halenda, P. P. *J. Am. Chem. Soc.* **1951**, *73*, 373.

(26) Sambrook, J.; Fritsch, E. F.; Maniatis, T. *Molecular Cloning: A laboratory Manual*; Cold Spring Harbor Lab. Press: Plainview, NY, 1989.

(27) Kneuer, C.; Sameti, M.; Haltner, E. G.; Schiestel, T.; Schirra, H.; Schmidt, H.; Lehr, C.-M. *Int. J. Pharm.* **2000**, *196*, 257.

(28) He, X.-X.; Kemin, W.; Tan, W.; Liu, B.; Lin, X.; He, C.; Li, D.; Huang, S.; Li, J. *J. Am. Chem. Soc.* **2003**, *125*, 7168.

(29) Radu, D. R.; Lai, C.-Y.; Jeftinija, K.; Rowe, E. W.; Jeftinija, S.; Lin, V. S.-Y. *J. Am. Chem. Soc.* **2004**, *126*, 13216.

(30) Dobrovolskaia, M. A.; McNeil, S. E. *Nat. Nanotechnol.* **2007**, *2*, 469.
(31) Kruk, M.; Hui, C. M. *Microporous Mesoporous Mater.* **2008**, *114*, 64.
(32) Kruk, M.; Hui, C. M. *J. Am. Chem. Soc.* **2008**, *130*, 1528.
(33) Schacht, S.; Janicke, M.; Schüth, F. *Microporous Mesoporous Mater.* **1998**, *22*, 485.
(34) Pauwels, B.; Van Tendeloo, G.; Thoelen, C.; Van Rhijn, W.; Jacobs, P. A. *Adv. Mater.* **2001**, *13*, 1317.
(35) Liu, S.; Cool, P.; Collart, O.; Van Der Voort, P.; Vansant, F. E.; Lebedev, O. I.; Van Tendeloo, G.; Jiang, M. *J. Phys. Chem. B* **2003**, *107*, 10405.
(36) Tan, B.; Rankin, S. E. *J. Phys. Chem. B* **2004**, *108*, 20122.
(37) Zhao, D.; Feng, J. L.; Huo, Q. S.; Melosh, N.; Fredrikson, G. H.; Chmelka, B. F.; Stucky, G. D. *Science* **1998**, *279*, 548.
(38) Schmidt-Winkel, P.; Yang, P.; Margolese, D. I.; Lettow, J. S.; Ying, J. Y.; Stucky, G. D. *Chem. Mater.* **2000**, *12*, 686.
(39) Lettow, J. S.; Han, Y. J.; Schmidt-Winkel, P.; Yang, P.; Zhao, D.; Stucky, G. D.; Ying, J. Y. *Langmuir* **2000**, *16*, 8291.
(40) Fan, J.; Yu, C.; Gao, F.; Lei, J.; Tian, B.; Wang, L.; Luo, Q.; Tu, Bo; Zhou, W.; Zhao, D. *Angew. Chem., Int. Ed.* **2003**, *42*, 3146.
(41) Yu, C. Z.; Fan, J.; Tian, B. Z.; Stucky, G. D.; Zhao, D. Y. *J. Phys. Chem. B* **2003**, *107*, 13368.
(42) Anderson, M. T.; Martin, J. E.; Odineck, J. G.; Newcomer, P. P. *Chem. Mater.* **1998**, *10*, 1490.
(43) Boissiere, C.; Martines, M. A. U.; Tokumoto, M.; Larbot, A.; Prouzet, E. *Chem. Mater.* **2003**, *15*, 509.
(44) Csögör, Z.; Nacken, M.; Sameti, M.; Lehr, C.-M.; Schmidt, H. *Mater. Sci. Eng., C* **2003**, *23*, 93.
(45) Roy, I.; Ohulchanskyy, T. Y.; Bharali, D. J.; Pudavar, H. E.; Mistretta, R. A.; Kaur, N.; Prasad, P. N. *Proc. Natl. Acad. Sci. U.S.A.* **2005**, *102*, 279.
(46) Chen, C.-C.; Liu, Y.-C.; Wu, C.-H.; Yeh, C.-C.; Su, M.-T.; Wu, Y.-C. *Adv. Mater.* **2005**, *17*, 404.
(47) Pearce, M. E.; Mai, H. Q.; Lee, N.; Larsen, S. C.; Salem, A. K. *Nanotechnology* **2008**, *19*, 175103.
(48) Corma, A. *Chem. Rev.* **1997**, *97*, 2373.
(49) Chen, C. Y.; Li, H. X.; Davis, M. E. *Microporous Mater.* **1993**, *2*, 17.
(50) Chen, C. Y.; Li, H. X.; Davis, M. E. *Microporous Mater.* **1993**, *2*, 27.
(51) Langowski, J.; Hammermann, M.; Klenin, K.; May, R.; Tóth, K. *Genetica* **1999**, *106*, 49.
(52) Mayan-Santos, M. D.; Marinez-Robles, M. L.; Hernandez, P.; Krimer, D.; Schvartzman, J. B. *Electrophoresis* **2007**, *28*, 3845.
(53) Deere, J.; Magner, E.; Wall, J. G.; Hodnett, B. K. *Chem. Commun.* **2001**, *5*, 465.
(54) Deere, J.; Magner, E.; Wall, J. G.; Hodnett, B. K. *J. Phys. Chem. B* **2002**, *106*, 7340.
(55) Zhang, H.; Sun, J.; Ma, D.; Bao, X.; Klein-Hoffmann, A.; Weinberg, G.; Su, D.; Schlögl, R. *J. Am. Chem. Soc.* **2004**, *126*, 7440.
(56) Zhang, H.; Sun, J.; Ma, D.; Weinberg, G.; Su, D. S.; Bao, X. *J. Phys. Chem. B* **2006**, *110*, 25908.
(57) Fan, J.; Lei, J.; Wang, L.; Yu, C.; Tu, B.; Zhao, D. *Chem. Commun.* **2003**, 2140.

JP807956R